CHAPTER III

GROWTH AND CHARACTERIZATION OF LHA SINGLE CRYSTAL

3.1 INTRODUCTION

Frequency conversion is an important technique for extending the useful wavelength range of lasers. In photonics, a growing need continues for low cost, highly nonlinear, efficient and high quality crystals for optical frequency conversion. Nonlinear optical (NLO) organic materials have received much importance for optical second harmonic generation (SHG) owing to their practical applications in the domain of optoelectronics and photonics. The search for suitable NLO materials exhibiting Second Harmonic Generation is the focus of current research. Amino acids are potential candidates for optical Second Harmonic Generation because they contain chiral carbon atom and crystallize in noncentro symmetric space groups (Senthil et al 2009, Senthil et al 2012 and Madhavan et al 2006). Salts of L-histidine have become promising NLO materials after Marcy et al. reported L-histidine tetrafluoborate has higher efficiency than the L-Arginine Phosphate (LAP) (Marcy H.O et al 1995). L-histidine acetate dihydrate (LHA) is one such organic nonlinear optical material that belongs to the histidine-complex family. L-histidine Acetate (LHA) has been reported as a promising organic NLO material, which has SHG efficiency three times higher than KDP (Madhavan et al 2007). In the present study, large size unidirectional LHA single crystal was grown successfully by SR method for the first time. Powder XRD, UV-Vis-NIR, microhardness, thermal and

dielectric studies were carried out to characterize the grown crystal. The NLO property of the crystal was confirmed by Kurtz powder technique.

3.2 EXPERIMENTAL PROCEDURE

The compound L-His.$CH_3COOH.2H_2O$ was synthesized by reacting equimolar proportion of L-histidine and acetic acid, in deionised water. The synthesized salt was purified by repeated crystallization. The seed crystal grown by the conventional slow solvent evaporation technique was used for the current study. <100> plane of the seed crystal of LHA was chosen and it was transferred to the saturated solution of LHA in the ampoule.

The experimental setup of SR method consists of growth ampoule made-up of glass with seed mounting pad. The circular shaped heaters were placed at the top and the bottom of the growth ampoule which provides the required experimental temperature for solvent evaporation (Sankaranarayanan et al 2006). The temperature around the growth ampoule is selected based on the solvent used and it is monitored with a temperature controller (40 ºC for top and 34 ºC for bottom).

Growth of highly transparent single crystal of LHA of 10 mm diameter and 28 mm length was grown in a period of 28 days and reported for the first time. The unidirectionaly grown LHA was shown in Fig. 3.1. The average growth rate was found to be nearly 1 mm per day. Thus it is found that the average growth rate of crystal by SR method was higher than the conventional method under prevailing conditions.

Fig.3.1. LHA crystal grown by SR method

3.3 RESULTS AND DISCUSSION

3.3.1 Powder XRD studies

The structural property of the grown crystal was studied by X-ray powder diffraction technique. Powder X-ray diffraction studies of LHA crystals were carried out, using RICH SIEFERT X-ray diffractometer with Cu K_α (λ = 1.5418Å) radiation. The samples were scanned for 2θ values from 10˚ to 50˚ at a rate of 2˚ /min.

Fig 3.2 shows the Powder XRD pattern of LHA crystal. The diffraction pattern of LHA crystal was indexed by least square fit method. The lattice parameter values of LHA crystal were calculated and are well matched with the reported literature. It is seen that the grown crystal crystallizes in triclinic P1 space group and the lattice parameters are shown in Table 3.1.

3.3.2 CHN analysis

For identifying the synthesized material, the CHN analysis was employed along with Powder X-ray diffraction (XRD) analyses. The elemental analysis of LHA was performed using Elementar Vario EL 111 Elemental analyzer. The theoretical and experimental atomic weight percentages are summarized in Table.3.2. Thus the chemical composition of LHA is established.

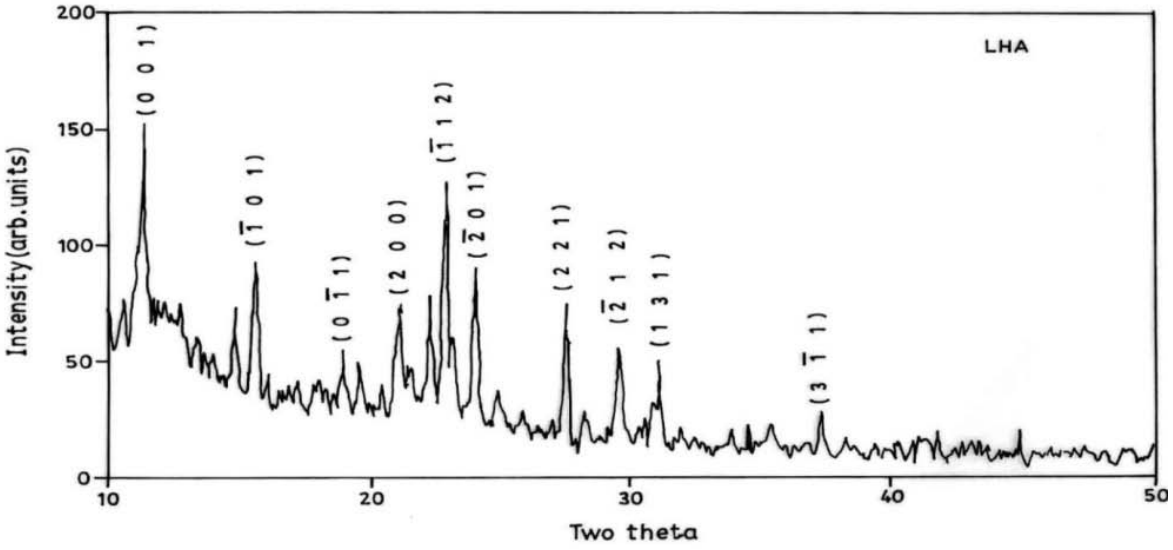

Fig.3.2. Powder XRD pattern of LHA crystal

Table. 3.1 Crystal data of LHA crystal

Empirical formula	$C_6N_3O_2H_{10}^{+}$ CH_3COO^{-} $.2H_2O$
Crystal system	Triclinic
Space group	P1
a(Å)	8.530
b(Å)	9.150
c(Å)	9.063
α°	61.73
β°	86.64
γ°	86.28
Volume $Å^3$	611.8

Table 3.2 Results of elemental analysis of LHA crystal

Molecular Weight: 251.24 g/mol		
Elements	Weight % composition	
	Theoretical	Experimental
C	38.25	38.41
H	6.82	6.91
N	16.73	16.79

3.3.3. Vibrational Spectrocopy

The FT-IR Spectrum of LHA was recorded in the range 450 cm^{-1} to 4000 cm^{-1}, using KBr pellet on BRUKKER IFS FT-IR Spectrometer (Fig 3.3). The polarized Fourier Transform Raman (FT-Raman) spectrum (Fig 3.4) was also recorded for the LHA crystal in order to qualitatively analyze the presence of functional groups in LHA.

O-H Vibrations

The O-H group vibrations are likely to be the most sensitive to the environment, so they show pronounced shifts in the spectra of the hydrogen bonded species. The hydroxyl stretching vibrations are generally (Sajan. D et al 2006) observed in the region around 3500 cm^{-1}. In the case of the un-substituted phenols it has been shown that the frequency of O-H stretching vibration in the gas phase is 3657 cm^{-1} (Michalska. D et al 1996). The O-H in-plane bending vibration in the phenols in general lies in the region 1150-1250cm^{-1} and is not much affected due to hydrogen bonding unlike to stretching and out – of – plane bending frequencies (Michalska. D et al 1996). However, for the associated molecule the O-H out-of-plane bending mode lies in the region 517-710 cm^{-1} in both inter molecular and intra molecular associations, the frequency is at a higher value in free O-H (Varsanyi. G et al, 1974). In the Raman spectrum the peak at 2933cm^{-1} is due to OH stretching.

C-H Vibrations

Presence of band in the region 2700-3000 cm^{-1} is the characteristic region for the identification of C-H stretching vibrations (Shanmugam. R et al

1984). In this region the bands are slightly affected by the nature of the substituents. The scaled vibrations are around 2800 cm^{-1}. The CH in-plane bending vibrations is generally observed in the region 1300-1000 cm^{-1}.For LHA molecule prominent number of CH in-plane bending vibrations are obtained at frequencies 1415, 1342, 1251 and 1147 cm^{-1} respectively. The absorption bands arising from C-H out-of-plane bending vibrations are usually observed in the region at 1000-675 cm^{-1} (Colthup. N. B et al 1990, Socrates. G et al 2001, Smith. B et al 1999). In the FT-Raman spectrum, asymmetric CH_2 stretching is observed at 1959 cm^{-1} and CH_3 asymmetric deformation is observed at 1482cm^{-1}.

N-H Vibrations

The N-H stretching vibrations generally give rise to bands at 3500-3300 cm^{-1} (Bellamy L.J et al 1975 and Spire A et al 2000). The peak at 3391 cm^{-1} confirms the presence of N-H vibration. In the FT-Raman spectrum the NH stretching of amino group is observed as a weak absorption at 3130 cm^{-1}.

Carboxly vibrations (COOH)

These stretching and bending vibrations of acid group are generally expected in the region 1400-1200 cm^{-1} (Roeges N.G.P et al 1994). The presence of strong absorption bands at 1634 and 1342 cm^{-1} confirmed the presence of COOH and COO^- groups in LHA crystals. The peak at 1634 cm^{-1} is due to C-O stretch of COOH and the aliphatic CH bend appears at 1342 cm^{-1}. The in-plane O-H deformation vibration usually appears as strong band in the

region 1440-1260 cm^{-1} (Chandraa S et al 2011). In the FT-Raman spectrum the peaks at 1278 cm^{-1},1417 cm^{-1} and 1628 cm^{-1} are for the C=O stretching of carboxylic group.

3.3.4 NLO studies

Kurtz SHG tests were carried out on the powdered sample of LHA using Nd:YAG Q-switched laser beam as a source (Kurtz et al 1968). For a laser input of 6.2mJ, the second harmonic signal (532 nm) of 91.66 mW and 352.48 mW were obtained for KDP and LHA respectively. Thus, the SHG efficiency of LHA is 3.8 times higher than that of KDP.

3.3.5 Laser Induced Damage Threshold study

Inorganic crystals are usually known to have high resistance to laser damage (Ramesh Babu et al 2006). In this section the results of laser induced damage threshold studies performed on LHA are presented. The laser damage threshold of LHA was carried out using laser setup in a single shot mode and it was found to be about 8.7 GW / cm^2, which indicates the suitability of this crystal for NLO applications.

3.3.6 UV-Vis-NIR spectrum

The optical absorption plays an important role in identifying the potential of the NLO material. Materials having wide absorption window with reduced absorption around the fundamental and second harmonic wavelength are of greater utility for NLO applications. Optical absorption data were taken on this polished crystal sample of about 4 mm thickness using a Varian carry 5E model dual beam spectrophotometer between 200 – 2000 nm.

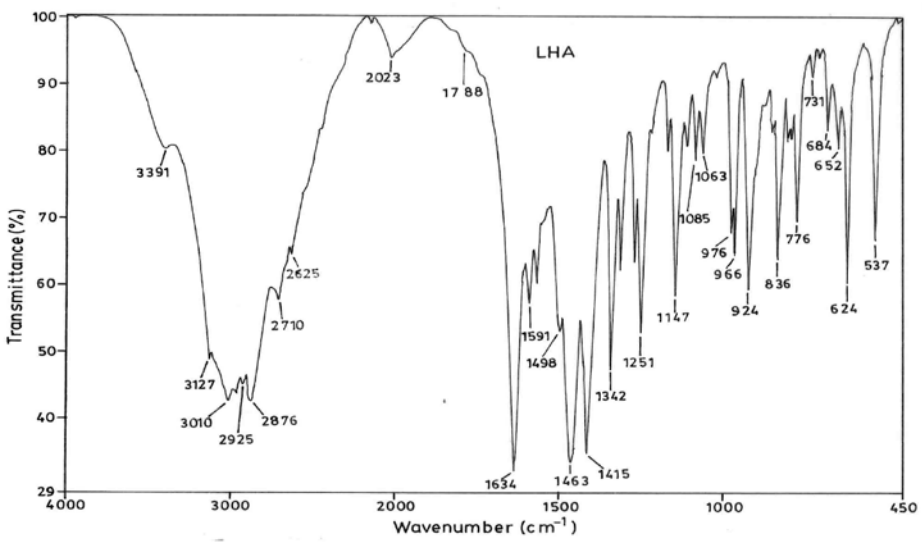

Fig 3.3 FT- IR spectrum of LHA

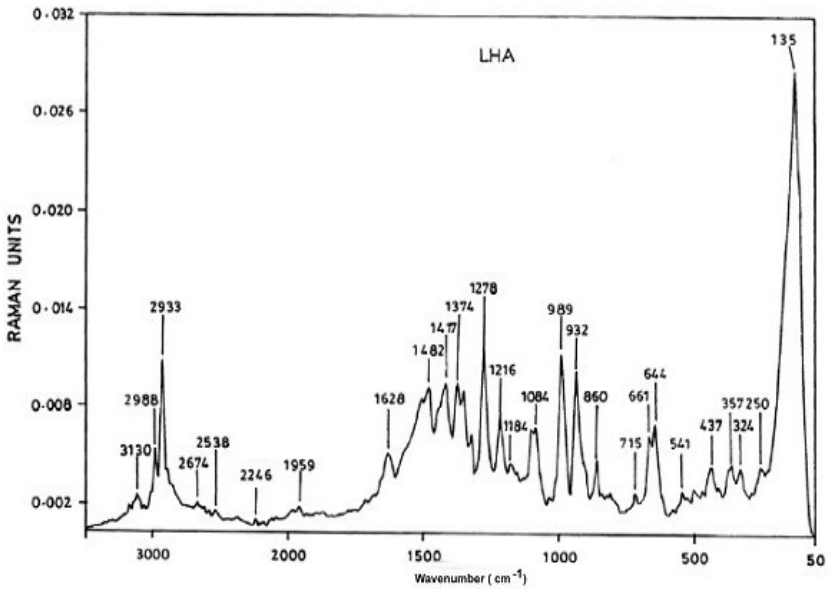

Fig 3.4 FT- RAMAN spectrum of LHA

The spectrum (Fig. 3.5) indicate that the LHA crystal have minimum absorption in the entire visible region. The required properties for NLO activity are minimum absorption and low cut-off wavelength which is evident in the grown crystal.

3.3.7 Microhardness test

Hardness of the material is a measure of resistance, it offers to deformation. Microhardness studies were carried out for the grown crystal using Leitz Wetzlar Vickers microhardness tester by varying the applied load from 5 g to 50 g. The indentation time was kept as 5s for all the loads. Fig. 3.6 shows the variations of Vickers hardness number with applied load. The value of work hardening coefficient is found to be 1.61. According to Onitsch, n lies between 1 and 1.6 for hard materials, and n is greater than 1.6 for soft materials. Hence, it is concluded that LHA crystal is a soft material.

3.3.8 Thermal studies

The TG and DTG analysis of LHA crystals were done in the nitrogen atmosphere in the temperature range ôC 28 -1000˚C using STA 409C instrument, at a heating rate of 10C/min. Fig. 3.7 shows the thermogram of the grown LHA. Due to the loss of lattice water, weight loss of about 35 % was observed for LHA between 115.5˚C and 274.6˚C. The total weight loss of 59 % was observed between 274.6 and 333˚C corresponds to the decomposition of pure LHA. 94% of the sample decomposes at a temperature more than 900 with around 6% as residue.

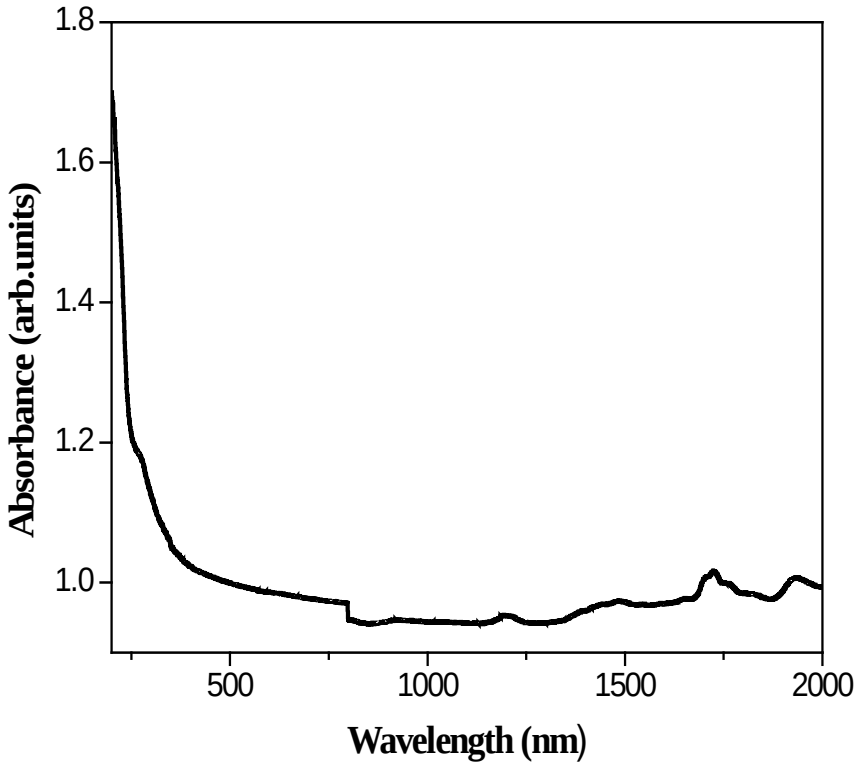

Fig.3.5 UV–Vis–NIR absorption spectrum of LHA

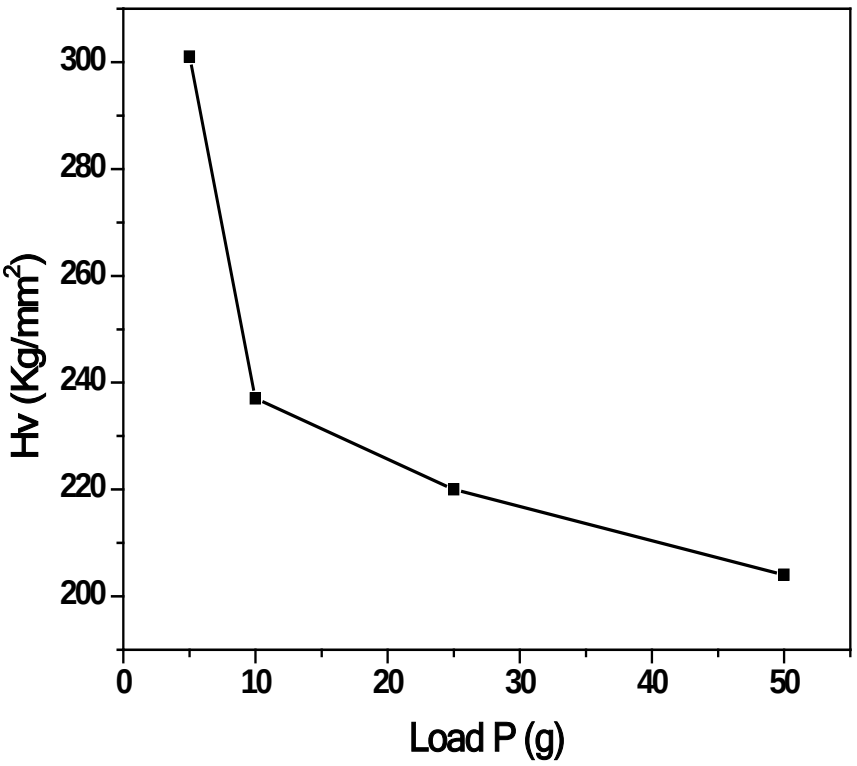

Fig 3.6. Vickers hardness profile of LHA

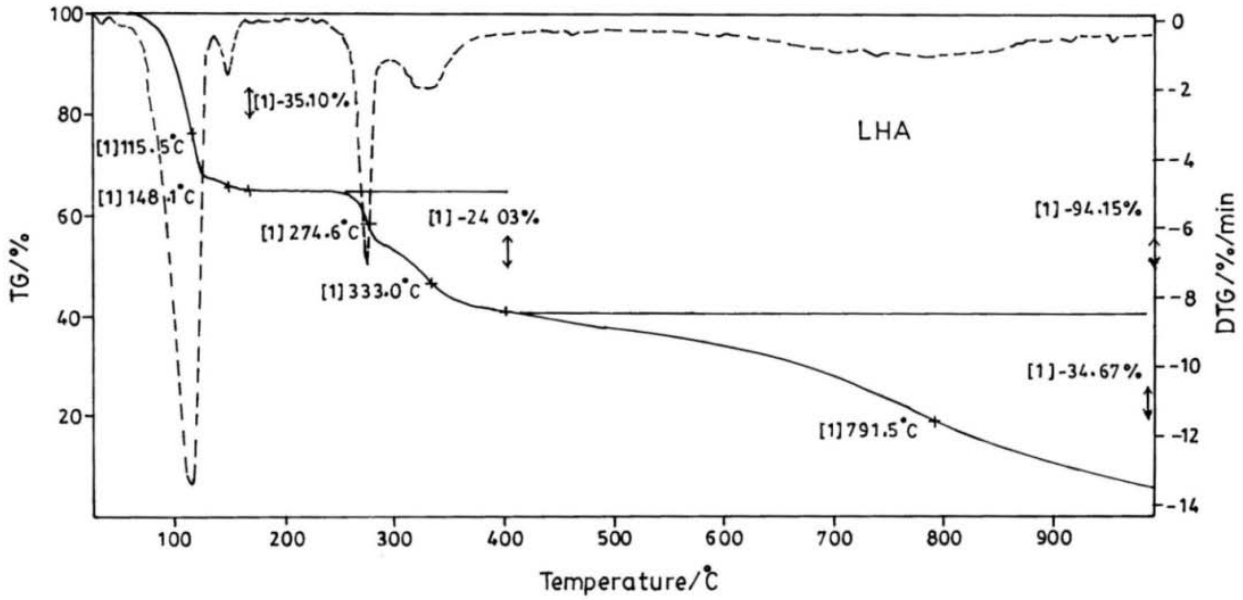

Fig.3.7. TGA and DTG thermogram of LHA crystal

3.3.9 Dielectric studies

Using the instrument, HIOKI 3532-50 LCR HITESTER, dielectric studies were carried out for the LHA crystal. Fig. 3.8 shows the variation of dielectric constant with frequency for the LHA crystal. The dielectric constant decreases with applied frequency. The high value of ε_r at low frequencies may be due to the presence of all the four polarizations namely; space charge, orientation, electronic and ionic polarizations and its low value at higher frequencies may be due to the loss of significance of these polarizations gradually. The variation of dielectric loss with frequency is shown in Fig. 3.9. As these materials shows low dielectric loss with high frequency, this sample possesses enhanced optical quality with lesser defects. This is an important parameter of vital importance for NLO materials in their application (Madhavan et al 2007).

3.3.10 Photoconductivity studies

Photoconductivity studies were carried out for LHA crystal using Keithley 485 picoammeter at room temperature. By connecting the samples to a DC power supply and a picoammeter, dark conductivity of the samples was studied. The light from the halogen lamp (100W) containing iodine vapor was focused on the sample with the help of a convex lens and the photo current of the sample was measured (Madhavan et al 2006). The DC input was increased from 200 V to 400 V in steps and the photo current was measured for the LHA sample.

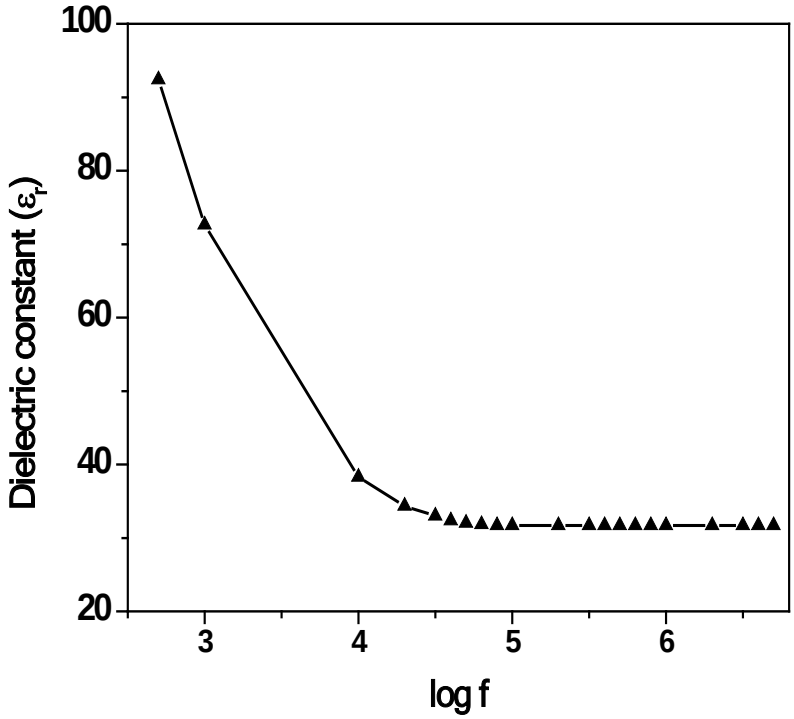

Fig 3.8. Plot of dielectric constant versus log frequency

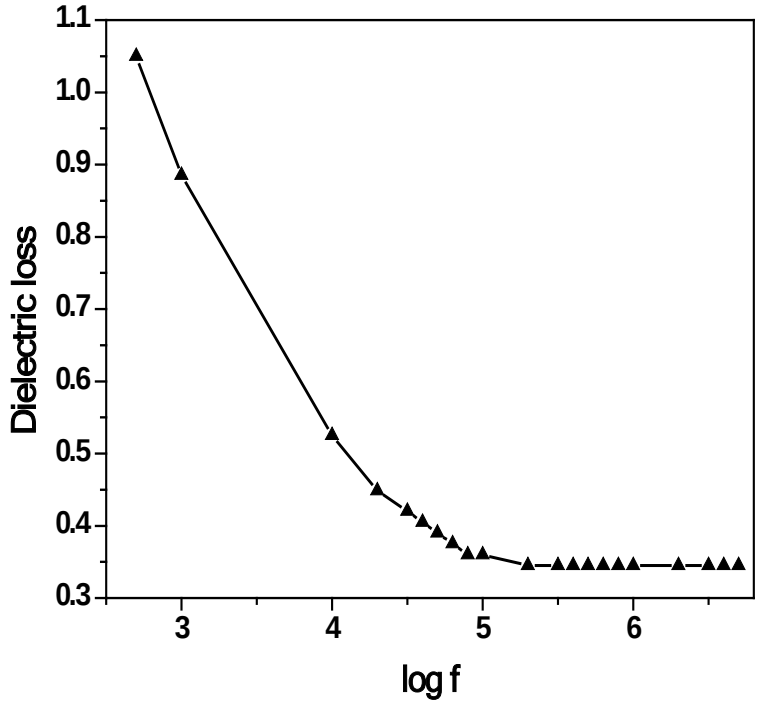

Fig 3.9. Plot of dielectric loss versus log frequency

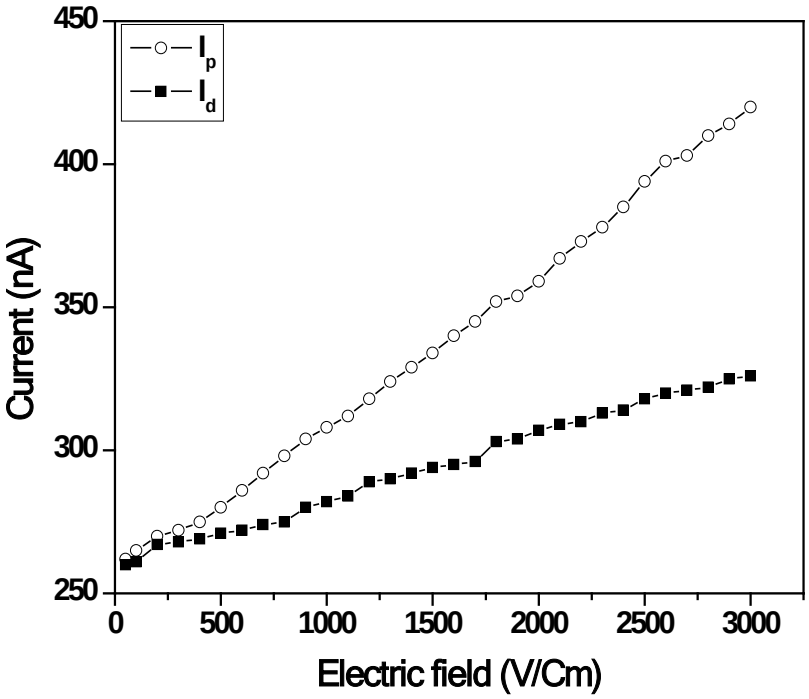

Fig 3.10. Photoconductivity of LHA

The variation of both dark current (I_d) and photo current (I_p) with applied field for LHA are shown in Fig. 3.10. It is seen from the plots that both I_d and I_p of the sample increase linearly with the applied field. It is also seen that the photo current of LHA crystal is always greater than the dark current and hence LHA exhibit positive photoconductivity. This phenomenon can be attributed to generation of mobile charge carriers caused by the absorption of photons (Cyrac Peter et al 2010).

3.4 CONCLUSION

Good quality unidirectional bulk crystal L-Histidine Acetate (LHA) was grown successfully by SR method. Powder X-ray diffraction studies were carried out, and the lattice parameters were calculated. The LHA crystal is transparent in the entire visible region, and has minimum absorption. The TGA studies show three stages of weight loss. From the dielectric studies it is seen that the dielectric constant and dielectric loss decreases with frequency. Photoconductivity studies reveal that LHA have positive photoconductivity. Hardness studies show that LHA is a soft material. NLO studies proved that LHA have second harmonic generation efficiency is 3.8 times that of KDP. The studies reveal that LHA could be a promising material for nonlinear device fabrication.